Hard Two-Photon Contribution to Elastic Lepton-Proton Scattering Determined by the OLYMPUS Experiment

B. S. Henderson,[1] L. D. Ice,[2] D. Khaneft,[3] C. O'Connor,[1] R. Russell,[1] A. Schmidt,[1] J. C. Bernauer,[1, *] M. Kohl,[4, †]
N. Akopov,[5] R. Alarcon,[2] O. Ates,[4] A. Avetisyan,[5] R. Beck,[6] S. Belostotski,[7] J. Bessuille,[1] F. Brinker,[8]
J. R. Calarco,[9] V. Carassiti,[10] E. Cisbani,[11] G. Ciullo,[10] M. Contalbrigo,[10] R. De Leo,[12] J. Diefenbach,[4]
T. W. Donnelly,[1] K. Dow,[1] G. Elbakian,[5] P. D. Eversheim,[6] S. Frullani,[11] Ch. Funke,[6] G. Gavrilov,[7] B. Gläser,[3]
N. Görrissen,[8] D. K. Hasell,[1] J. Hauschildt,[8] Ph. Hoffmeister,[6] Y. Holler,[8] E. Ihloff,[1] A. Izotov,[7] R. Kaiser,[13]
G. Karyan,[8, ‡] J. Kelsey,[1] A. Kiselev,[7] P. Klassen,[6] A. Krivshich,[7] I. Lehmann,[13] P. Lenisa,[10] D. Lenz,[8]
S. Lumsden,[13] Y. Ma,[3] F. Maas,[3] H. Marukyan,[5] O. Miklukho,[7] R. G. Milner,[1] A. Movsisyan,[5, §] M. Murray,[13]
Y. Naryshkin,[7] R. Perez Benito,[3] R. Perrino,[12] R. P. Redwine,[1] D. Rodríguez Piñeiro,[3] G. Rosner,[13] U. Schneekloth,[8]
B. Seitz,[13] M. Statera,[10] A. Thiel,[6] H. Vardanyan,[5] D. Veretennikov,[7] C. Vidal,[1] A. Winnebeck,[1] and V. Yeganov[5]

(The OLYMPUS Collaboration)

[1]*Massachusetts Institute of Technology, Cambridge, MA, USA*
[2]*Arizona State University, Tempe, AZ, USA*
[3]*Johannes Gutenberg-Universität, Mainz, Germany*
[4]*Hampton University, Hampton, VA, USA*
[5]*Alikhanyan National Science Laboratory (Yerevan Physics Institute), Yerevan, Armenia*
[6]*Rheinische Friedrich-Wilhelms-Universität, Bonn, Germany*
[7]*Petersburg Nuclear Physics Institute, Gatchina, Russia*
[8]*Deutsches Elektronen-Synchrotron, Hamburg, Germany*
[9]*University of New Hampshire, Durham, NH, USA*
[10]*Università degli Studi di Ferrara and Istituto Nazionale di Fisica Nucleare sezione di Ferrara, Ferrara, Italy*
[11]*Istituto Nazionale di Fisica Nucleare sezione di Roma and Istituto Superiore di Sanità, Rome, Italy*
[12]*Istituto Nazionale di Fisica Nucleare sezione di Bari, Bari, Italy*
[13]*University of Glasgow, Glasgow, United Kingdom*
(Dated: December 19, 2016)

The OLYMPUS collaboration reports on a precision measurement of the positron-proton to electron-proton elastic cross section ratio, $R_{2\gamma}$, a direct measure of the contribution of hard two-photon exchange to the elastic cross section. In the OLYMPUS measurement, 2.01 GeV electron and positron beams were directed through a hydrogen gas target internal to the DORIS storage ring at DESY. A toroidal magnetic spectrometer instrumented with drift chambers and time-of-flight scintillators detected elastically scattered leptons in coincidence with recoiling protons over a scattering angle range of $\approx 20°$ to $80°$. The relative luminosity between the two beam species was monitored using tracking telescopes of interleaved GEM and MWPC detectors at $12°$, as well as symmetric Møller/Bhabha calorimeters at $1.29°$. A total integrated luminosity of 4.5 fb^{-1} was collected. In the extraction of $R_{2\gamma}$, radiative effects were taken into account using a Monte Carlo generator to simulate the convolutions of internal bremsstrahlung with experiment-specific conditions such as detector acceptance and reconstruction efficiency. The resulting values of $R_{2\gamma}$, presented here for a wide range of virtual photon polarization $0.456 < \epsilon < 0.978$, are smaller than some hadronic two-photon exchange calculations predict, but are in reasonable agreement with a subtracted dispersion model and a phenomenological fit to the form factor data.

Measurements of the proton's elastic form factor ratio, $\mu_p G_E^p/G_M^p$, using polarization techniques [1–8] show a dramatic discrepancy with the ratio obtained using the traditional Rosenbluth technique in unpolarized cross section measurements [9–14]. One hypothesis for the cause of this discrepancy is a contribution to the cross section from hard two-photon exchange (TPE), which is not included in standard radiative corrections and would affect the two measurement techniques differently [15–

20]. Standard radiative correction prescriptions account for two-photon exchange only in the soft limit, in which one photon carries negligible momentum [21, 22]. There is no model-independent formalism for calculating hard TPE. Some model-dependent calculations suggest that TPE is responsible for the form factor discrepancy [17–20] while others contradict that finding [23, 24].

Hard TPE can be quantified from a measurement of $R_{2\gamma}$, the ratio of positron-proton to electron-proton elas-

tic cross sections that have been corrected for the standard set of radiative effects, including soft TPE. The interference of one- and two-photon exchange is odd in the sign of the lepton charge, so any deviation in $R_{2\gamma}$ from unity can be attributed to hard TPE. The OLYMPUS experiment, as well as two recent experiments at VEPP-3 [25] and CLAS [26], have measured $R_{2\gamma}$ to specifically determine if hard TPE is sufficient to explain the observed discrepancy in the proton's form factor ratio, or if some additional explanation is needed.

Both the magnitude of $R_{2\gamma}$ and its kinematic dependence are relevant. If hard TPE is the cause of the discrepancy, phenomenological models [27–30] predict $R_{2\gamma}$ should rise with decreasing ϵ and increasing Q^2. Here, ϵ is the virtual photon polarization parameter given by $[1 + 2(1 + \tau)\tan^2(\theta_e/2)]^{-1}$, where θ_e is the lepton scattering angle and $\tau = Q^2/(4M_p^2)$, where M_p is the proton mass, and $Q^2 = -q_\mu q^\mu$ is the negative four-momentum transfer squared.

Only a brief overview of the OLYMPUS experiment is given here (see [31] for a detailed description). The OLYMPUS experiment took data in the last running of the DORIS electron/positron storage ring at DESY, Hamburg, Germany. The DORIS magnet power supplies were modified to allow the beam species to be changed daily. The experiment collected a total integrated luminosity of 4.5 fb^{-1}. The 2.01 GeV stored beams with up to 65 mA of current passed through an internal, unpolarized hydrogen gas target with an areal density of approximately 3×10^{15} atoms/cm^2 [32].

The detector was based on the former MIT-Bates BLAST detector [33]: a toroidal magnetic spectrometer with the two horizontal sections instrumented with large acceptance ($20° < \theta < 80°$, $-15° < \phi < 15°$) drift chambers (DC) for 3D particle tracking and walls of time-of-flight scintillator bars (ToF) for triggering and particle identification. To a good approximation, the detector system was left-right symmetric and this was used as a cross-check in the analysis. Most of the data were collected with positive toroid polarity to avoid excessive noise rates in the DC due to low-energy electrons being bent away from the beam axis into the DCs.

Two new detector systems were designed and built to monitor the luminosity. These were symmetric Møller/Bhabha calorimeters (SYMB) at 1.29° [34] and two telescopes of three triple gas electron multiplier (GEM) detectors [35] interleaved with three multi-wire proportional chambers (MWPC) mounted at 12°.

The trigger system selected candidate events that resulted from a lepton and proton detected in coincidence in opposite sectors. The CBELSA/TAPS data acquisition system [36] was used to readout the data and stored it to disk.

An optical survey of all detector positions was made and the magnetic field was mapped throughout the tracking volume [37].

A complete Monte Carlo (MC) simulation of the experiment was developed in order to account for the differences between electrons and positrons with respect to radiative effects, changing beam position and energy, the spectrometer acceptance, track reconstruction efficiency, luminosity, and elastic event selection. Rather than correct each effect individually, the simulation allowed the complete forward propagation of the correlations amongst all of these effects. The ratio we report is given by

$$R_{2\gamma} = \left[\frac{N_{\exp}(e^+)}{N_{\exp}(e^-)}\right] \Big/ \left[\frac{N_{\mathrm{MC}}(e^+)}{N_{\mathrm{MC}}(e^-)}\right] = \frac{R^{\exp}}{R^{\mathrm{MC}}}, \quad (1)$$

where N_i are the observed and simulated counts.

The first stage in the simulation was a radiative event generator developed specifically for OLYMPUS [30, 38]. This generator produced lepton-proton events weighted by several different radiative cross section models. In this letter, the results from four prescriptions are presented: following Mo-Tsai [21] and Maximon-Tjon [22], both with radiative effects to order α^3 and to all orders through exponentiation. The Mo-Tsai order α^3 prescription is equivalent to the ESEPP generator [39] used by the VEPP-3 experiment. The difference in $R_{2\gamma}$ extracted using the four approaches is as much as 1.5% at low ϵ, indicating that higher-order effects in radiative corrections are significant and depend on the effective cutoff energy.

Particle trajectories were simulated using a three-dimensional model of the apparatus and then digitized to produce simulated data in exactly the same format as the experimental data. This digitization procedure accounted for the efficiency and resolution of individual detector elements, determined using data-driven approaches. Both the experimental and simulated data were analyzed with the same analysis code.

Track reconstruction was performed using a pattern matching procedure on detector signals to identify track candidates. Then two distinct tracking algorithms were employed to fit the track initial conditions: momentum, scattering angles, and vertex position.

Four independent elastic event selection routines were developed [30, 38, 40, 41], and the results presented are the average of the four with the statistical uncertainty calculated as the average of the statistical uncertainty of each analysis. Two additional routines are in preparation [42, 43]. Each routine uses different approaches, but all leverage the fact that the kinematics of elastic events is over-determined so that cuts on reconstructed kinematic quantities—momenta, angles, time-of-flight, vertex positions of the lepton and proton—could be used to reduce background from the sample of elastic events. Time-of-flight was used effectively to discriminate leptons from protons. Cuts on the proton acceptance were used to avoid acceptance edge effects. All of the routines utilized a background subtraction procedure, and all confirmed that the background rates were similar for electron and

TABLE I. Contributions to the systematic uncertainty in $R_{2\gamma}$.

Correlated contributions	Uncertainty in $R_{2\gamma}$
Beam energy	0.04–0.13%
MIE luminosity	0.36%
Beam and detector geometry	0.25%
Uncorrelated contributions	
Tracking efficiency	0.20%
Elastic selection and background subtraction	0.25–1.17%

positron modes. Background typically varied from negligible at low Q^2 to $\approx 20\%$ at high Q^2. The routines binned elastic events according to the reconstructed proton angle, as this reconstruction was identical in electron and positron modes. We report results on a subset of the total recorded data selected for optimal running conditions, corresponding to 3.1 fb^{-1} of integrated luminosity.

The integrated luminosity for each beam species was independently monitored using the 12° telescopes, the SYMB, and from the beam current and target density recorded by the slow control system. The most accurate determination came from an analysis of multi-interaction events (MIE) in the SYMB [30, 44]. In the MIE analysis, the luminosity was extracted from the ratio of rates of two types of events. The denominator was the rate of symmetric Møller/Bhabha events, in which the two final state leptons entered the SYMB. The numerator was the rate of events in which a beam lepton scattered elastically from a target proton and entered the calorimeter in random coincidence with a symmetric Møller/Bhabha interaction. By extracting the luminosity from a ratio of rates, the MIE analysis exploited cancelations of several systematic uncertainties (like acceptance, detector efficiency, etc.), reducing the uncertainty in the relative luminosity between beam species to 0.36%.

The redundant pair of tracking telescopes at 12° measured elastic ep scattered leptons in coincidence with recoil protons in the DC and ToF around 72°, which permitted a measurement of $R_{2\gamma}$ at $\epsilon = 0.978$ with negligible statistical uncertainty using the MIE luminosity [40].

Table I summarizes the dominant contributions to the systematic uncertainty in $R_{2\gamma}$. The uncertainty from geometry was estimated from the differences between $R_{2\gamma}$ extracted from left-lepton versus right-lepton events. The uncertainty from tracking efficiency was estimated from the performance of the two different tracking algorithms. The uncertainty from elastic selection was estimated from the variance in $R_{2\gamma}$ produced by the different selection routines.

We want to emphasize that radiative corrections have a large effect on the OLYMPUS determination of $R_{2\gamma}$. The corrections to $R_{2\gamma}$ are driven by the lepton charge-odd corrections: soft TPE and the interference of bremsstrahlung off the lepton and proton. In the OLYM-

PUS analysis, radiative effects cannot be unfolded from the effects of detector efficiency, acceptance, etc., but the magnitude of radiative effects on $R_{2\gamma}$ can be estimated by comparing the full simulation with one where the events are re-weighted by the first Born approximation. Figure 1 shows the size of the correction for the four different prescriptions. We find that the corrections are approx-
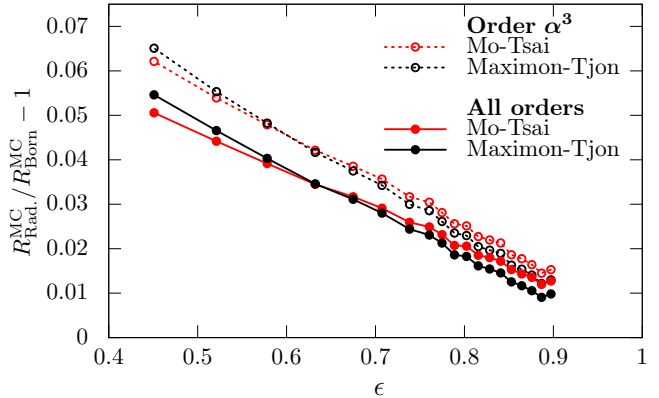
FIG. 1. Approximate effects of radiative corrections versus ϵ are on the order of several percent.

imately 5–6% at the lowest ϵ values, and, furthermore, that higher-order effects can alter the correction by as much as 1%. The effective energy cut-off in the analysis is only a few percent of the outgoing lepton energy. In that range, the exponentiation should yield a more accurate result. The large dependency on the prescription used underscores that theoretical improvements to the treatment of higher order bremsstrahlung are crucial for future high-precision experiments.

The OLYMPUS determination of $R_{2\gamma}$ as a function of ϵ and Q^2 is provided in Table II for the four different radiative correction prescriptions. The results using Mo-Tsai to all orders are shown in Fig. 2, along with theoretical calculations by Blunden [45] and by Tomalak [46] and the phenomenological prediction from Bernauer's [29] fit to unpolarized and polarized proton form factors measurements that includes a parameterization for the TPE ϵ and Q^2 dependence. OLYMPUS finds that the contribution from hard TPE is small at this beam energy though there is a noticeable trend from below unity at higher values of ϵ increasing to around 2% at $\epsilon = 0.46$. The results are in general below the theoretical prediction of Blunden. The subtracted dispersion calculation of Tomalak shown has used Bernauer's form factor data and a subtraction point at $\epsilon = 0.5$. Both Tomalak's calculation and Bernauer's phenomenological prediction are in reasonable agreement with the OLYMPUS results.

A comparison of the results from recent $R_{2\gamma}$ experiments to Blunden's newest calculation $(N + \Delta)$ is shown in Fig. 3. We plot the difference between the data and theory calculated at the ϵ and Q^2 for each data point to approximately take into account that the data were

$\langle\epsilon\rangle$	$\langle Q^2\rangle$ $\frac{\text{GeV}^2}{c^2}$	$R_{2\gamma}$ (a)	$R_{2\gamma}$ (b)	$R_{2\gamma}$ (c)	$R_{2\gamma}$ (d)	$\delta_{\text{stat.}}$	$\delta_{\text{syst.}}^{\text{uncorr}}$ $\times 10^{-4}$	$\delta_{\text{syst.}}^{\text{corr}}$
0.978	0.165	0.9971	0.9967	0.9979	0.9978	3	46	36
0.898	0.624	0.9920	0.9948	0.9944	0.9958	19	37	45
0.887	0.674	0.9888	0.9913	0.9912	0.9923	21	42	45
0.876	0.724	0.9897	0.9927	0.9921	0.9935	23	60	45
0.865	0.774	0.9883	0.9921	0.9907	0.9929	26	50	45
0.853	0.824	0.9879	0.9918	0.9903	0.9926	29	39	45
0.841	0.874	0.9907	0.9952	0.9931	0.9958	32	42	45
0.829	0.924	0.9919	0.9967	0.9943	0.9972	36	33	45
0.816	0.974	0.9950	0.9998	0.9973	1.0002	39	33	45
0.803	1.024	0.9913	0.9969	0.9936	0.9971	43	40	45
0.789	1.074	0.9905	0.9955	0.9927	0.9956	47	50	45
0.775	1.124	0.9904	0.9960	0.9926	0.9960	52	41	45
0.761	1.174	0.9950	1.0011	0.9971	1.0009	57	63	45
0.739	1.246	0.9945	1.0007	0.9964	1.0002	46	56	45
0.708	1.347	0.9915	0.9985	0.9930	0.9977	54	49	46
0.676	1.447	0.9842	0.9912	0.9854	0.9899	63	50	46
0.635	1.568	1.0043	1.0126	1.0049	1.0105	63	55	46
0.581	1.718	0.9968	1.0063	0.9966	1.0032	77	96	46
0.524	1.868	0.9953	1.0055	0.9941	1.0013	95	118	46
0.456	2.038	1.0089	1.0212	1.0064	1.0154	104	108	46

TABLE II. OLYMPUS results for $R_{2\gamma}$ using the prescriptions: Mo-Tsai to order α^3 (a) and to all orders (b); and using Maximon-Tjon to order α^3 (c) and to all orders (d).
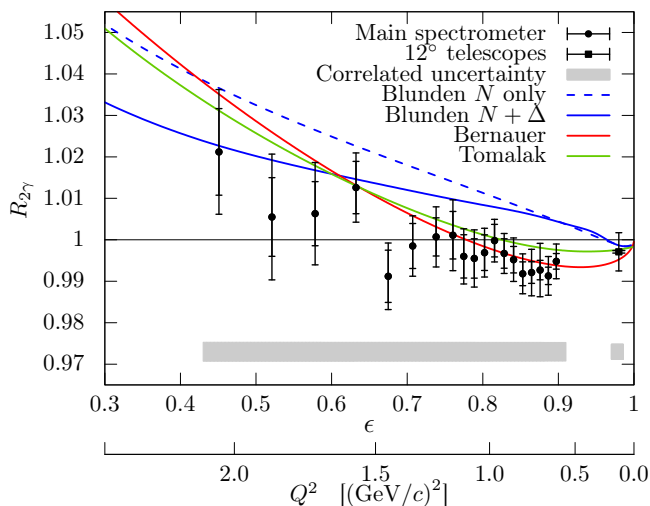

FIG. 2. OLYMPUS result for $R_{2\gamma}$ using the Mo-Tsai [21] prescription for radiative corrections to all orders. Uncertainties shown are statistical (inner bars), uncorrelated systematic (added in quadrature, outer bars), and correlated systematic (gray band). Note the 12° data point at $\epsilon = 0.978$ is completely dominated by systematic uncertainties.

taken at different ϵ and Q^2 values. This shows the data are largely consistent with each other, but mostly below the calculation by Blunden. A similar plot could be made versus Q^2. Comparison with the phenomenological prediction of Bernauer (not shown) shows good agreement.

We do not agree with the conclusions of the earlier papers [25, 26]. The data shown in Fig. 3 clearly favours a
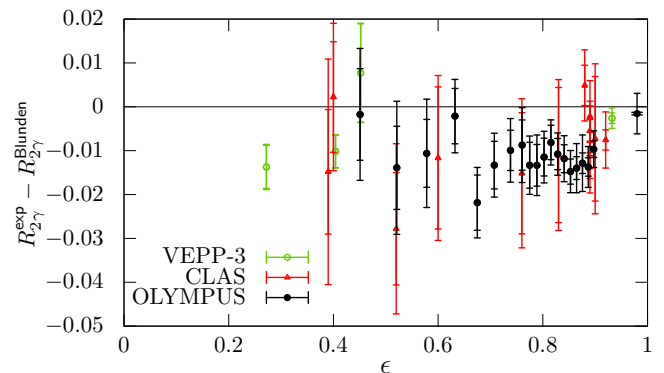

FIG. 3. Comparison of the recent results to the calculation by Blunden. The data are in good agreement, but generally fall below the prediction. Please note that data at similar ϵ values have been measured at different Q^2. Also note that the VEPP-3 data have been normalized to the calculation at high ϵ.

smaller $R_{2\gamma}$. While the agreement with the phemonological prediction of Bernauer suggests that TPE is causing most of the discrepancy in the form factor ratio in the measured range. The theoretical calculation of Blunden, which shows roughly enough strength to explain the discrepancy at larger Q^2, does not match the data in this regime. To clarify the situation, the size of TPE at large Q^2 has to be determined in future measurements.

* Corresponding author: bernauer@mit.edu
† Corresponding author: kohlm@jlab.org; partially supported by Jefferson Lab
‡ Also with Alikhanyan National Science Laboratory (Yerevan Physics Institute), Yerevan, Armenia
§ Also with Università degli Studi di Ferrara and Istituto Nazionale di Fisica Nucleare sezione di Ferrara, Ferrara, Italy

[1] B. Hu et al., Phys. Rev. **C73**, 064004 (2006).
[2] G. MacLachlan et al., Nucl. Phys. **A764**, 261 (2006).

[3] O. Gayou *et al.*, Phys. Rev. **C64**, 038202 (2001).

[4] V. Punjabi *et al.*, Phys. Rev. **C71**, 055202 (2005).

[5] M. K. Jones *et al.*, Phys. Rev. **C74**, 035201 (2006).

[6] A. J. R. Puckett *et al.*, Phys. Rev. Lett. **104**, 242301 (2010).

[7] M. Paolone *et al.*, Phys. Rev. Lett. **105**, 072001 (2010).

[8] A. J. R. Puckett *et al.*, Phys. Rev. **85**, 045203 (2012).

[9] J. Litt *et al.*, Phys. Lett. **B31**, 40 (1970).

[10] W. Bartel *et al.*, Nucl. Phys. **B58**, 429 (1973).

[11] L. Andivahis *et al.*, Phys. Rev. **D50**, 5491 (1994).

[12] R. C. Walker *et al.*, Phys. Rev. **D49**, 5671 (1994).

[13] M. E. Christy *et al.*, Phys. Rev. **C70**, 015206 (2004).

[14] I. A. Qattan *et al.*, Phys. Rev. Lett. **94**, 142301 (2005).

[15] P. A. M. Guichon and M. Vanderhaeghen, Phys. Rev. Lett. **91**, 142303 (2003).

[16] P. G. Blunden, W. Melnitchouk, and J. A. Tjon, Phys. Rev. Lett. **91**, 142304 (2003).

[17] Y. C. Chen *et al.*, Phys. Rev. Lett. **93**, 122301 (2004).

[18] A. V. Afanasev *et al.*, Phys. Rev. **D72**, 013008 (2005).

[19] P. G. Blunden, W. Melnitchouk, and J. A. Tjon, Phys. Rev. **C72**, 034612 (2005).

[20] S. Kondratyuk, P. G. Blunden, W. Melnitchouk, and J. A. Tjon, Phys. Rev. Lett. **95**, 172503 (2005).

[21] L. W. Mo and Y.-S. Tsai, Rev. Mod. Phys. **41**, 205 (1969).

[22] L. C. Maximon and J. A. Tjon, Phys. Rev. **C62**, 054320 (2000).

[23] Yu. M. Bystritskiy, E. A. Kuraev, and E. Tomasi-Gustafsson, Phys. Rev. **C75**, 015207 (2007).

[24] E. A. Kuraev, V. V. Bytev, S. Bakmaev, and E. Tomasi-Gustafsson, Phys. Rev. **C78**, 015205 (2008), arXiv:0710.3699 [hep-ph].

[25] I. A. Rachek *et al.*, Phys. Rev. Lett. **114**, 062005 (2015).

[26] D. Adikaram *et al.*, Phys. Rev. Lett. **114**, 062003 (2015).

[27] Y.-C. Chen, C.-W. Kao, and S.-N. Yang, Phys. Rev. **B652**, 269 (2007).

[28] J. Guttmann, N. Kivel, M. Meziane, and M. Vanderhaeghen, Eur. Phys. Jour. **A47**, 1 (2011).

[29] J. C. Bernauer *et al.* (A1), Phys. Rev. **C90**, 015206 (2014).

[30] A. Schmidt, Ph.D. thesis, Massachusetts Institute of Technology, Cambridge, Massachusetts (2016).

[31] R. Milner, D. K. Hasell, M. Kohl, U. Schneekloth, *et al.*, Nucl. Instr. Meth. **A741**, 1 (2014).

[32] J. C. Bernauer *et al.*, Nucl. Instr. Meth. **A755**, 20 (2014).

[33] D. K. Hasell *et al.*, Nucl. Instr. Meth. **A603**, 247 (2009).

[34] R. Perez Benito *et al.*, Nucl. Instr. Meth. **A826**, 6 (2016).

[35] O. Ates, Ph.D. thesis, Hampton University, Hampton, Virginia (2014).

[36] A. Thiel *et al.*, Phys. Rev. Lett. **109**, 102001 (2012), arXiv:1207.2686 [nucl-ex].

[37] J. C. Bernauer *et al.*, Nucl. Instr. Meth. **A823**, 9 (2016).

[38] R. L. Russell, Ph.D. thesis, Massachusetts Institute of Technology, Cambridge, Massachusetts (2016).

[39] A. V. Gramolin *et al.*, J. Phys. **G41**, 115001 (2014).

[40] B. S. Henderson, Ph.D. thesis, Massachusetts Institute of Technology, Cambridge, Massachusetts (2016).

[41] J. C. Bernauer, "Elastic event selection," (2016), unpublished.

[42] C. O'Connor, Ph.D. thesis, Massachusetts Institute of Technology, Cambridge, Massachusetts (2017).

[43] L. D. Ice, Ph.D. thesis, Arizona State University, Tempe, Arizona (2016).

[44] A. Schmidt *et al.*, Nucl. Instr. Meth. (2016), to be published.

[45] P. Blunden, Private communication. (2016).

[46] O. Tomalak and M. Vanderhaeghen, Eur. Phys. J. **A51**, 24 (2015), arXiv:1408.5330 [hep-ph].